Supporting Information

3D-printed hollow microneedle-based electrochemical sensor for wireless glucose monitoring

Chuchu Chen[1,†], Yonghao Fu[1,†], Yuehe Lin[1], Yun Liu[2], Dan Du[1,3,], Kaiyan Qiu[1,*]*

[1] School of Mechanical Engineering, Washington State University, Pullman, Washington 99164, United States

[2] Research School of Chemistry, Australian National University, Canberra, ACT 2601, Australia

[3] Department of Pharmaceutical Sciences, College of Pharmacy and Pharmaceutical Sciences, Washington State University, Spokane, Washington 99202, United States

* Corresponding authors.

† These authors contributed equally to this work.

E-mail: kaiyan.qiu@wsu.edu; annie.du@wsu.edu;

Keywords: wearable electrochemical sensor; single-atom nanozyme; hollow microneedle array; wireless glucose monitoring, resin 3D printing

Table of Contents

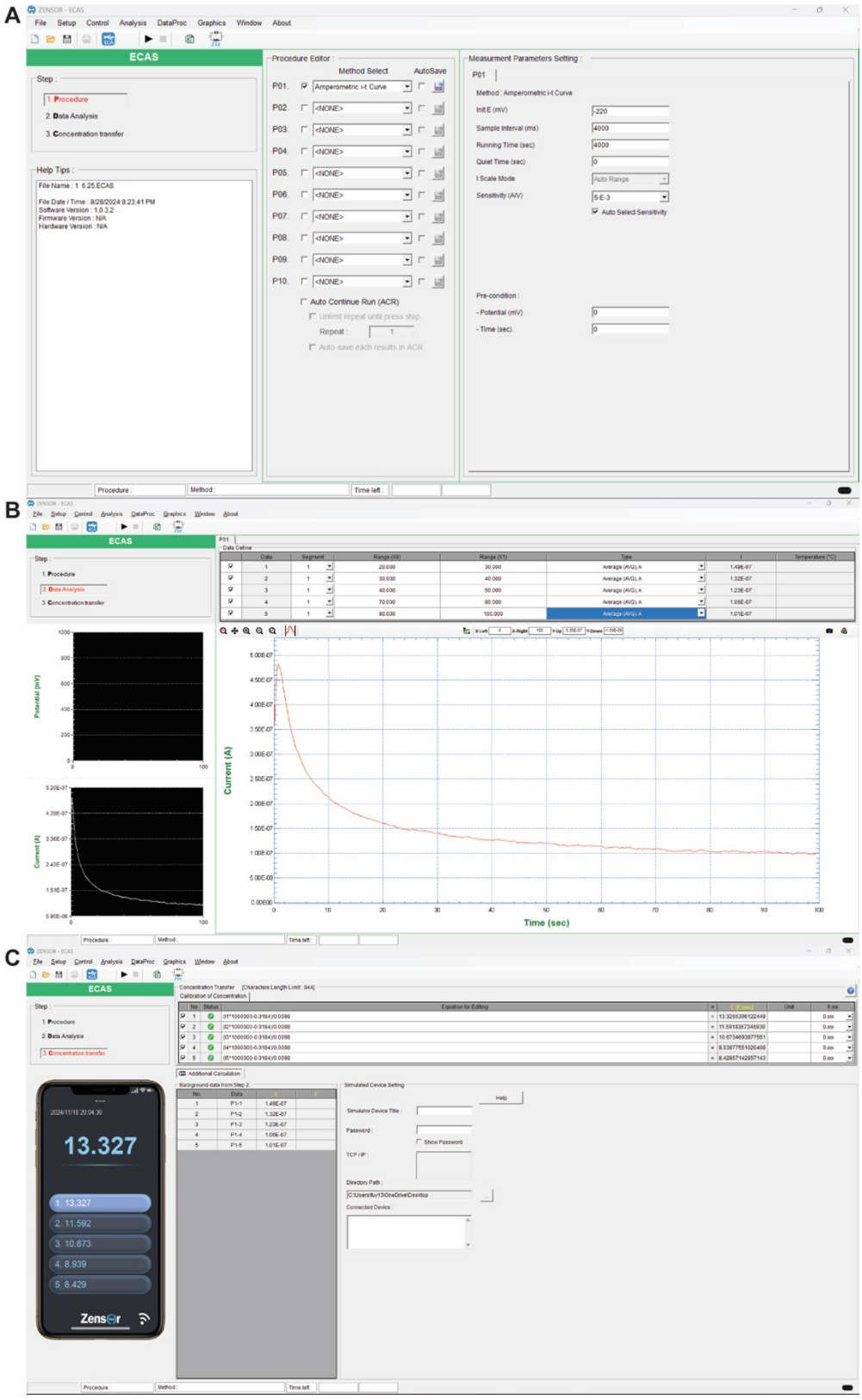

Figure S1. **The settings in the EIWP 110 software.** A) Procedure settings; B) Data analysis settings; C) Concentration transfer settings.

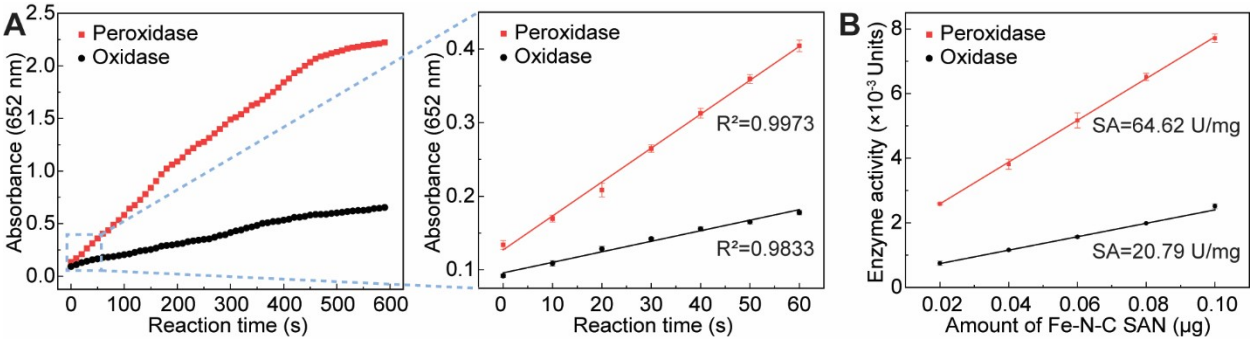

Figure S2. **Enzyme activity characteristics of Fe-N-C SANs.** A) The absorbance-reaction time curve of the TMB chromogenic reaction catalyzed by the Fe-N-C SANs; B) The enzyme specific activity of Fe-N-C SANs. All data are shown as mean ± SD (n = 3).

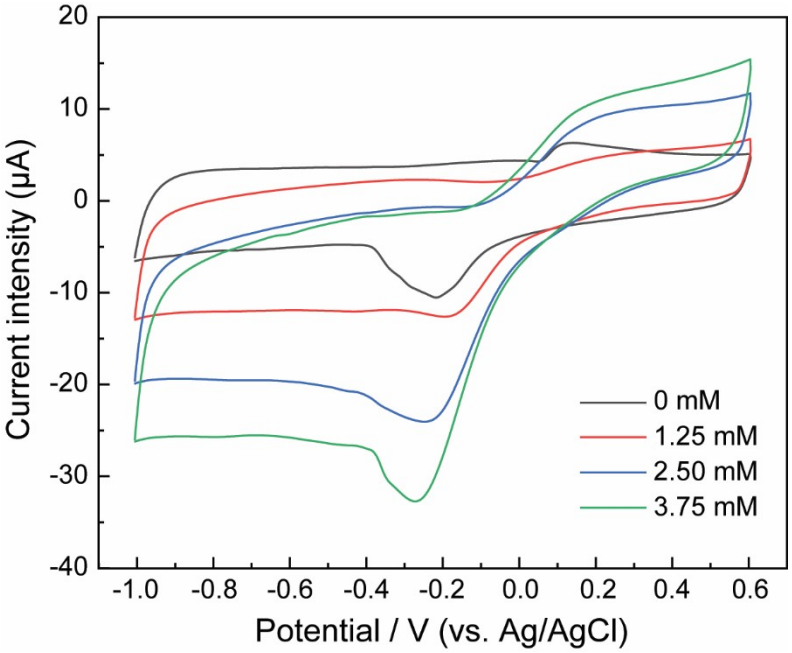

Figure S3. **The cyclic voltammetry of Fe-N-C SACs-modified SPE in PBS solution with 0, 1.25, 2.5 and 3.75 mM H_2O_2.**

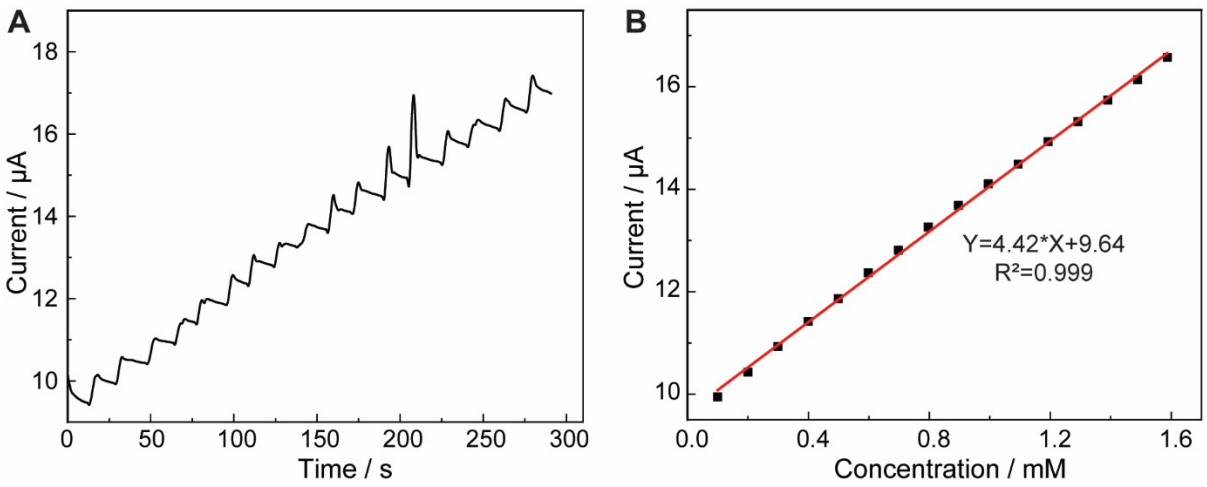

Figure S4. **Continuous detection of H_2O_2 by Fe-N-C SACs-modified electrod**e. A) Amperometry curve of Fe-N-C SACs during the continuous addition of H_2O_2 in PBS solution at an applied potential of -0.2 V; B) Linear relationship between H_2O_2 concentration and response current.

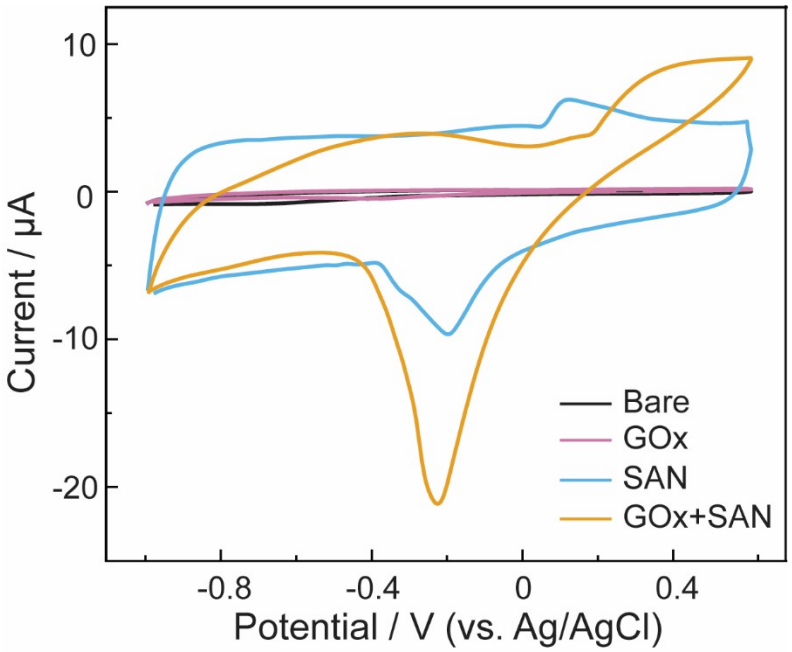

Figure S5. Cyclic voltammetry curves of bare, GOx-coated, SANs-coated and SANs/GOx-coated SPE in 2.5 mM glucose solution.

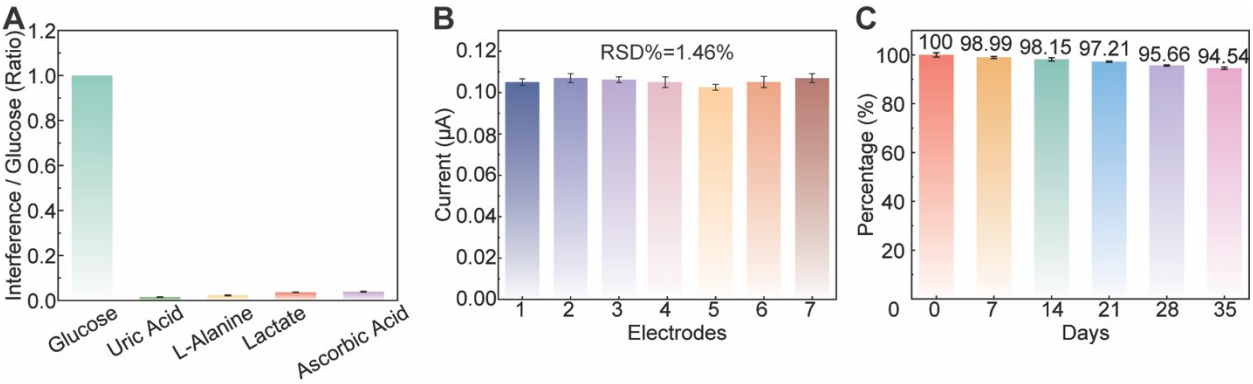

Figure S6. **The anti-interference, reproducibility and stability of SAN/GOx-coated SPEs.** A) The ratio of the current response of 5 mM interferences at -0.2V using amperometry to the current response of glucose at some concentration; B) The response current of 2 mM glucose measured by seven electrodes. Relative standard deviation (RSD) is 1.46% and there was no significant difference among the seven electrodes ($P>0.05$); C) Measurement performance of the electrode after room temperature storage. The measurement time was 7th day, 14th day, 21st day, 28th day and 35th day after the start of room temperature storage. All data are shown as mean ± SD (n = 3).

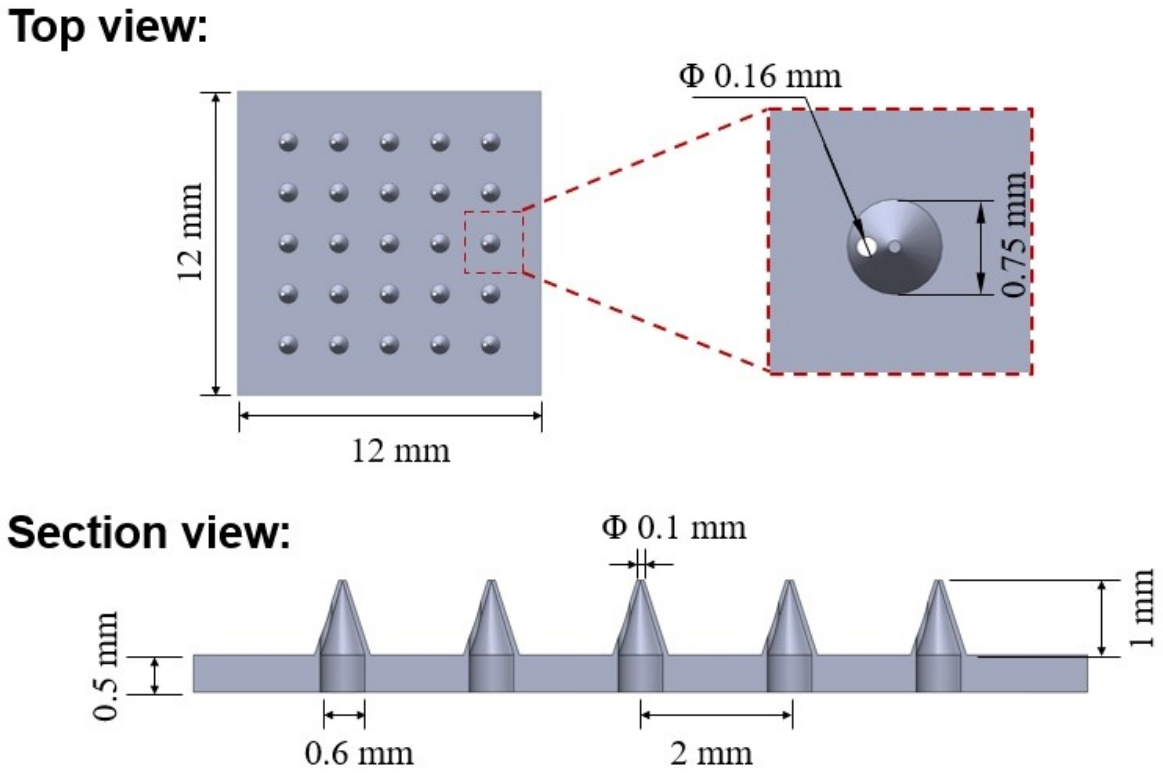

Figure S7. Dimensional specifications of the microneedle array from the top view and section view.

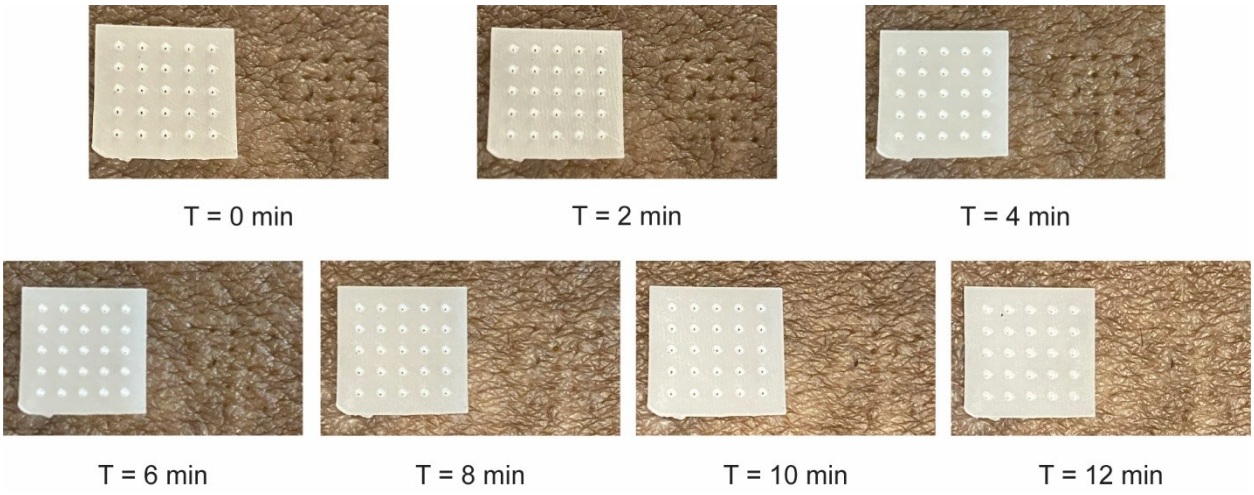

Figure S8. **Time-lapse images of porcine skin after microneedle array insertion.** Images were taken at 0, 2, 4, 6, 8, 10 and 12 min after insertion.

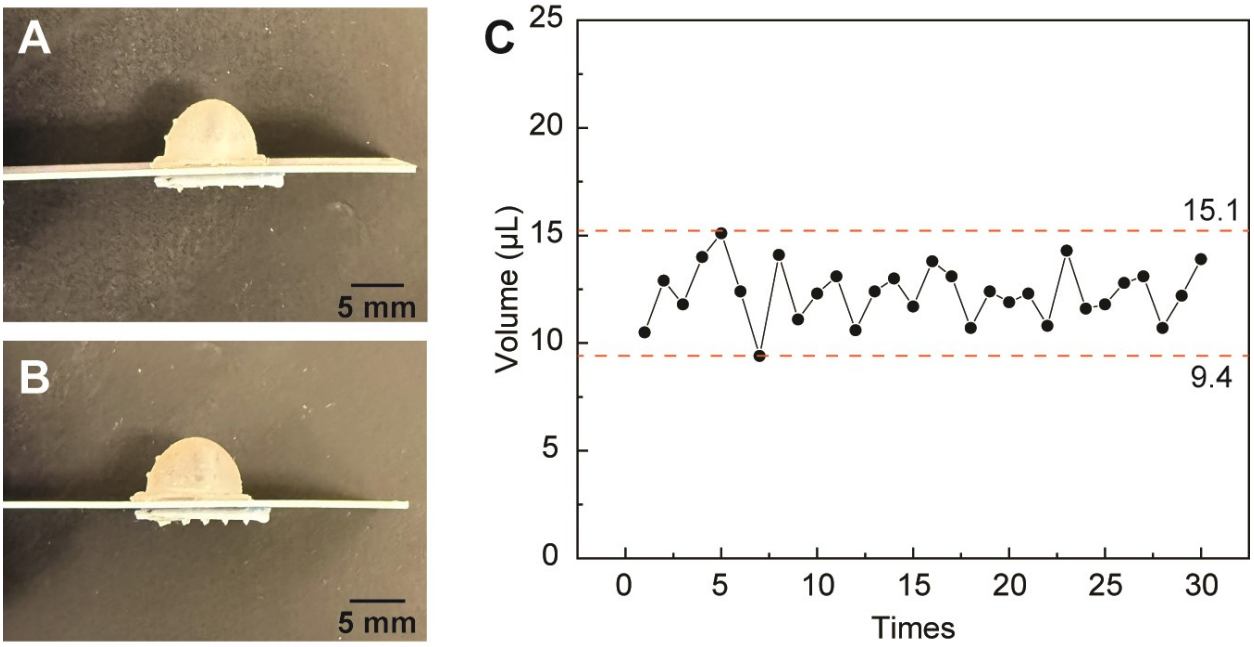

Figure S9. Stability evaluation of the finger-activated pump within the 3D-printed electrochemical biosensing platform. A) Pump image before use. B) Pump image after 100 extraction cycles. C) Extraction volume per cycle from skin-mimicking model.

Table S1. Comparison of the detection performance of the hollow microneedle (HMN)-based single-atom nanozyme (SAN)/glucose oxidase (GOx)-modified glucose sensor with other reported materials-modified glucose sensors.

Sensor	linear range/mM	Limit of detection/μM	Ref.
ERGO-PLL	0.005-0.05	2	[1]
RGO-PtNW	0.032-1.89	4.6	[2]
RGO/CuSNFs	0.001-2	0.19	[3]
CoFe-NG	0-3.25	37.7	[4]
CoPC/graphene/IL	0.01-13 & 1.3-5.0	0.67	[5]
GOx@PAVE-CNTs	1-5	0.36	[6]
AuNPs@g-C_3N_4	5-100	1.2	[7]
GOx/Chitosan/Au-Ti	0.04-15.05	1.75	[8]
Co_3O_4/graphene nanocomposite	0.016-1.3	0.5	[9]
FTO-CNTs/PEI/GOx	0.07-0.7	70	[10]
GOx/Au@C/TiO_2/FTO	0.1-1.6	49	[11]
GOx-SiO_2/Lig/CPE	0.5-9	145	[12]
Nafion/GOx/ZnO NRs/ITO	0.05-1	60	[13]
Cu_2O	0.1-1	12	[14]
SAN/GOx	**0.0001-0.1 & 0.1-50**	**0.285**	**This work**

Table S2. Comparison of the detection performance of the hollow microneedle-based single-atom nanozyme/glucose oxidase-modified electrochemical glucose sensor with other microneedle-based glucose sensors.

Microneedle based-sensor	linear range/mM	Limit of detection/μM	Ref.
Polymeric microneedle-based glucose sensor	0-31.45	1.8	[15]
Silicon microneedle array patch	1-9	660	[16]
Wearable hollow microneedle sensing patches	2.5-22.5	/	[17]
Microneedle array sensor	0.05-20	19.4	[18]
Microneedle-enabled electrochemical sensor	0.1-100	33.3	
Electrochemical microneedle sensor	0-20	/	[19]
3D-printed hollow microneedle-based electrochemical sensor	**0.0001-0.1 & 0.1-50**	**0.285**	**This work**

Table S3. Results of detection by SAN/GOx-modified glucose sensor in artificial ISF and Skin-mimicking model.

Reference values/mM	Sensor values/mM	Sensor recovery/%
Artificial ISF		
0.98	1.01	103.29
5.08	5.22	102.84
10.6	10.89	102.71
20.05	20.59	102.70
Skin-mimicking phantom gel		
1	1.01	101.02
2	1.95	97.49
5	5.14	102.86
10	9.82	98.16
15	15.83	105.51
20	19.70	98.52

Movie S1. Demonstration of the Finger-activated Pump Extraction Process in the 3D-printed Electrochemical Biosensing Platform.

References

1. D. Zhang, X. Chen, W. Ma, T. Yang, D. Li, B. Dai and Y. Zhang, *Materials Science and Engineering: C*, 2019, **104**, 109880.
2. X. Fu, Z. Chen, S. Shen, L. Xu and Z. Luo, *International Journal of Electrochemical Science*, 2018, **13**, 4817-4826.
3. X. Yan, Y. Gu, C. Li, B. Zheng, Y. Li, T. Zhang, Z. Zhang and M. Yang, *Analytical Methods*, 2018, **10**, 381-388.
4. M. Janyasupab and C. Promptmas, 2018 IEEE-EMBS Conference on Biomedical Engineering and Sciences (IECBES), 2018.
5. S. Chaiyo, E. Mehmeti, W. Siangproh, T. L. Hoang, H. P. Nguyen, O. Chailapakul and K. Kalcher, *Biosensors and Bioelectronics*, 2018, **102**, 113-120.
6. S. Xu, Y. Zhang, Y. Zhu, J. Wu, K. Li, G. Lin, X. Li, R. Liu, X. Liu and C.-P. Wong, *Biosensors and Bioelectronics*, 2019, **135**, 153-159.
7. N. Wu, Y.-T. Wang, X.-Y. Wang, F.-N. Guo, H. Wen, T. Yang and J.-H. Wang, *Analytica Chimica Acta*, 2019, **1091**, 69-75.
8. W. Lipińska, K. Siuzdak, J. Karczewski, A. Dołęga and K. Grochowska, *Sensors and Actuators B: Chemical*, 2021, **330**, 129409.
9. T.-T. Wang, X.-F. Huang, H. Huang, P. Luo and L.-S. Qing, *Advanced Sensor and Energy Materials*, 2022, **1**, 100016.
10. M.-H. Lin, S. Gupta, C. Chang, C.-Y. Lee and N.-H. Tai, *Microchemical Journal*, 2022, **180**, 107547.
11. L. Ge, R. Hou, Y. Cao, J. Tu and Q. Wu, *RSC Advances*, 2020, **10**, 44225-44231.
12. A. Jędrzak, T. Rębiś, Ł. Klapiszewski, J. Zdarta, G. Milczarek and T. Jesionowski, *Sensors and Actuators B: Chemical*, 2018, **256**, 176-185.
13. N. S. Ridhuan, K. Abdul Razak and Z. Lockman, *Sci Rep*, 2018, **8**, 13722.
14. F. F. Franco, R. A. Hogg and L. Manjakkal, *Biosensors*, 2022, **12**, 174.
15. M. S. Reza, H. Song, Y. Lee, M. Asaduzzaman, C. Cha and J. Y. Park, 2023.
16. M. Dervisevic, M. Alba, L. Yan, M. Senel, T. R. Gengenbach, B. Prieto-Simon and N. H. Voelcker, *Advanced Functional Materials*, 2022, **32**, 2009850.
17. M. Parrilla, U. Detamornrat, J. Domínguez-Robles, R. F. Donnelly and K. De Wael, *Talanta*, 2022, **249**, 123695.
18. K. B. Kim, W.-C. Lee, C.-H. Cho, D.-S. Park, S. J. Cho and Y.-B. Shim, *Sensors and Actuators B: Chemical*, 2019, **281**, 14-21.
19. T. Ming, T. Lan, M. Yu, X. Duan, S. Cheng, H. Wang, J. Deng, D. Kong, S. Yang and Z. Shen, *Microchemical Journal*, 2024, **207**, 112021.